



## XRD analysis and surface roughness of AL2024 alloy produced through P/M route and machined by using CNC milling machine

Y. Rameswara Reddy\* and K. Pavankumar Reddy

*Department of Mechanical Engineering, JNTUACEP, Pulivendula, Constitute College of Jawaharlal Nehru Technological University Anantapur, Ananthapuramu, India.*

Open Access Research Journal of Engineering and Technology, 2023, 04(02), 036–045

Publication history: Received on 28 April 2023; revised on 09 June 2023; accepted on 12 June 2023

Article DOI: <https://doi.org/10.53022/oarjet.2023.4.2.0063>

### Abstract

The purpose of this analysis is to examine the surface roughness during machining of aluminum 2024 prepared through the powder metallurgical (P/M) route. Aluminium 2024 alloy is prepared with different compositions, such as pure Al, 1.5 W% of Mg, and 2–6% of Cu powders. Powders are blended with the ball milling machine according to the composition required, and green compacts are prepared in a square-shaped die (25\*25mm) by applying a uniaxial load of 250 Mpa  $\pm$ 50. The sintering process was performed at a temperature of 594 °C for 60 minutes, and the heating profile consisted of a 10-minute isothermal keep at 594 °C followed by cooling in Furness. It presents and addresses compaction characteristics, green density, dimensional changes during sintering, sintering density, mechanical properties, and microstructures. Also determined were the surface roughness and MRR during machining with a CNC milling machine at different depths of cut.

**Keywords:** CNC Milling; Al2024; P/M; XRD; SEM; Surface roughness; MRR

### 1. Introduction

The technique of powder metallurgy is well known for the manufacture of near-net-shape goods. The materials have been used for the manufacture of internal combustion engines and the automobile industry, thereby minimising the preliminary and operating costs [1]. Any of these products are still mass-produced for the car industry. The growth of this sector is on the rise over the coming years [2].

In the 1990s, after cam shaft bearing caps were originally produced for original automotive machinery producers such as General Engines and Daimler Chrysler, the aluminum powder metallurgy process was improved. Products are now routinely produced on a single engine schedule in annual quantities of more than 107 units per year [3], [4].

The majority of APM component implementations are focused on designing mechanical properties with substantial geometric complexity and close-dimensional tolerances. Pump gears, retainer frames, connecting rods, camshaft bearing cups, variable cam phasers, and thrust plates, to name just a few, are among the increasingly popular APM alloy parts. Each new application is accompanied by specifications for tensile and compressive mechanical properties, density, stiffness, and fatigue tolerance requirements [5]–[8].

For researchers, the study of the microstructural characterization and mechanical properties of 2024 aluminum alloys is largely intense [3], [9]–[11]. The aim of this work is to determine the surface roughness and MRR during machining of aluminum 2024 prepared through the powder metallurgical (P/M) route.

\* Corresponding author: Y. Rameswara Reddy

## 2. Material and method

### Raw materials Used

The following raw materials were used to build the 2024 aluminum alloy:

- Aluminum (Al) powder, supplied by plating chemicals of 98 percent purity and standard 270  $\mu\text{m}$  particle size
- Copper (Cu) has a gross particle size of 100 $\mu\text{m}$  and a purity of 99.0%.
- The purity of magnesium (Mg) is 99.8 percent, and the mean particle size is 100  $\mu\text{m}$ .

On the basis of Al weight percentage, the alloy metal powder compositions are selected and shown in Table 1.

**Table 1** Chemical composition of the specimens

Sample	Composition In Weight Percent
1	Pure Al
2	Al-1.5%Mg
3	Al- 1.5%Mg - 2%Cu
4	Al- 1.5%Mg -3%Cu
5	Al- 1.5%Mg -4%Cu
6	Al- 1.5%Mg -5%Cu
7	Al- 1.5%Mg -6%Cu

### 2.1. Blending

The proportion of aluminium oxide was calculated using the component composition. All of these powders are mixed together using planetary ball milling at 300 RPM using tungsten carbide balls, and the particle size is checked using a particle size analyzer.

### 2.2. Compaction

By using 100 tonnes of hydraulic pressure, the powders are compacted into a square shape having 25\*25\*9 mm sizes at a pressure of 200  $\pm$ 50 Mpa according to the given compositions shown in Table 1. During compaction, to avoid friction between powder particles and the die surface, zinc stearate was used.

### 2.3. Sintering

Sintering characteristics were originally studied under a laboratory box furnace in ranges of 590  $^{\circ}\text{C} \pm 20$   $^{\circ}\text{C}$  for 60 minutes. All preforms are coated with ceramics to avoid oxidation and have been heated up to 594  $^{\circ}\text{C}$ . Sintering temperature at a 10  $^{\circ}\text{C}$  per minute heating rate, and then after 24 hours, the furnace cooled to room temperature.

### 2.4. EDX and XRD Analysis

The scanning electron microscope (SEM) "JEOL-JSM 500" was used to do a microstructural analysis of the alloys. It has been inspected for alloys ranging from 10, 20, 50, 100, 200, and 500  $\mu\text{m}$ . An energy dispersive x-ray (EDX) analyzer fitted with a used SEM conducted chemical scrutiny of the sintered sample. The x-ray diffraction (XRD) of the MINI FLEX 600 was conducted to determine the crystal structure of crystalline materials/alloys. The purpose of the research was to find atomic structures using the powder diffraction technique.

### 2.5. Experimental Setup

The MTAB XL Mill CNC milling machine is utilised in these tests to perform the milling operation on all preforms that are manufactured using the powder metallurgy approach. It is a three-axis CNC milling machine. The 28 trials are carried out on the work material while maintaining a constant speed and feed while varying the depth of cut, as indicated in the picture below. Surface roughness and material removal rate are two output parameters that are chosen. Figure 1 shows the experimental setup.



**Figure 1** Experimental setup

### 3. Results and Discussions

The development of the structural elements of the aluminum powder metallurgy technique can be accomplished in many different ways. These phases are equivalent to both compaction and sintering methods. The volume variations in green and sintered compacts, composition of compounds, crystal structures, rate of material removal, and compact surface roughness are discussed below.

#### 3.1. Compaction Characteristics

With a compaction pressure ranging from 150 to 200 Mpa, the compaction properties of the 2024 Aluminium alloy were investigated. In figure 2, a graphic representation of the compaction thickness of the square elemental 2024 Aluminium alloy is presented. Depending on the material's composition, the compaction of Aluminium alloys has a green thickness. As indicated in figure 2, the maximum thickness of sample 4 (Al, 3% Cu, and 1.5% Mg) was calculated.

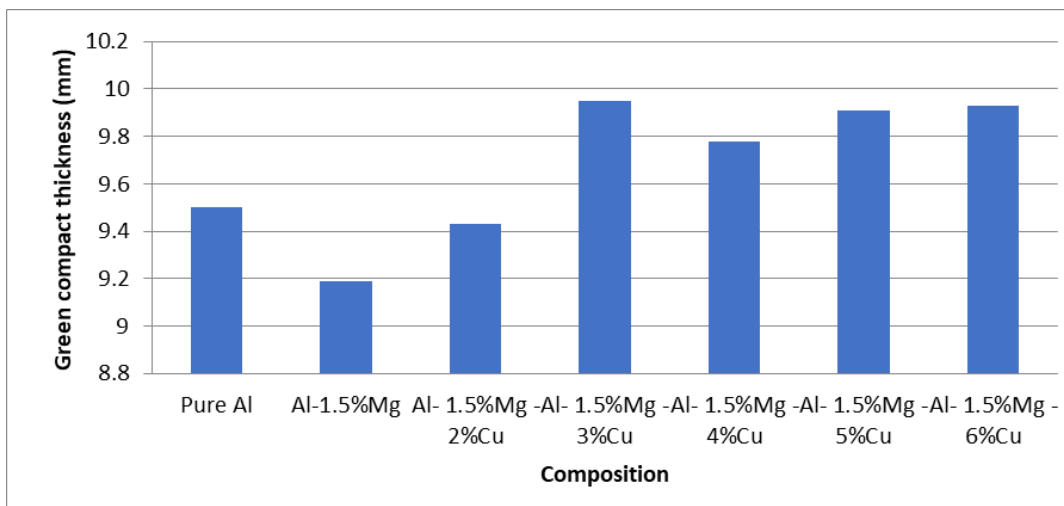


**Figure 2** Compacted specimens' thickness

#### 3.2. Sintering Characteristic

Square specimens of the Aluminium 2024 alloy were sintered in the open at 594 °C for 1 hour and held isothermal at 590 °C for 10 minutes. Usage of ceramic coatings to reduce oxidation in comparison to the green compacts in figure 2 & 3, the thickness of the components reduces during sintering. Sintered Aluminium 2024 powder metallurgical compacts now have less porosity. Due to the low melting temperature, the components underwent fast dimensional changes during sintering.

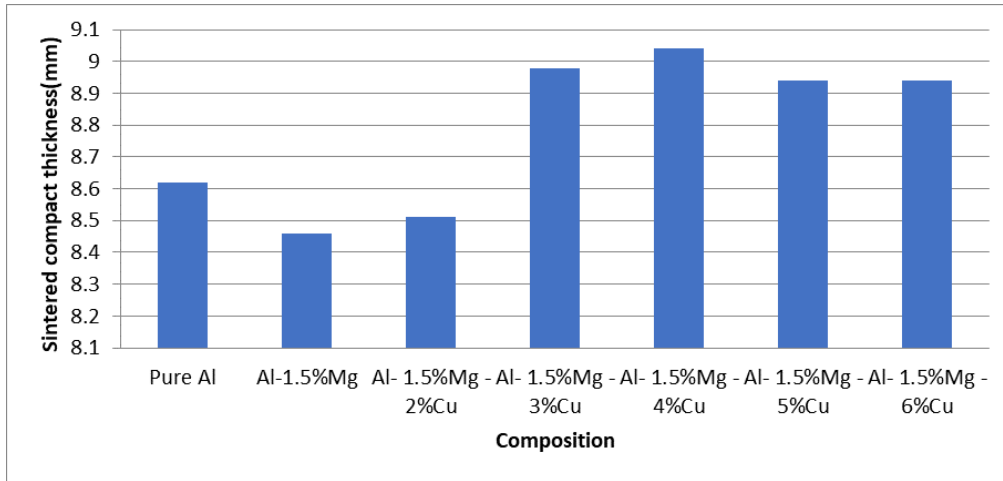


**Figure 3** Sintered specimen's thickness

### 3.3. Shrinkage Characteristics

The volume percentage increases for Aluminum 2024 powder metallurgical alloy when sintered in an open-air atmospheric box furnace at 594 °C for an hour. Heating is essential for removing or decreasing the specimen's pores and oxides. Volume shrinkage was discovered in this experiment when compared to green components, particularly the thickness of sintered components. When comparing figure 2 & 3 it can be clearly observed .

### 3.4. Cooling Time and Sintering Time

The sintering temperature in the heating phase is 30 °C/minute in this study. The sintering time is 60 °C/minute in the cooling profile. The graphs were seen between the heating time of sintering and the cooling time of sintering. As demonstrated in figure 4.

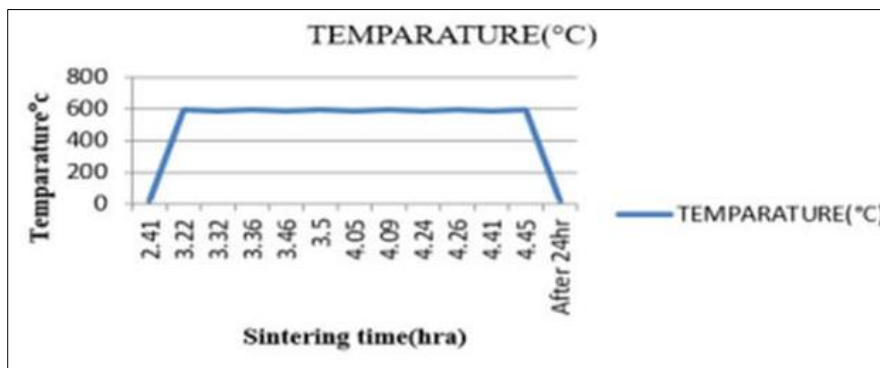


**Figure 4** Cooling and heating time of sintering

### 3.5. EDX Analysis

The scanning electron microscope (SEM) equipped with an EDX analyzer is used for chemical composition analysis purposes. In an EDX examination, find out the material percentages in aluminum 2024 alloy specimens as shown in figures 5 to 11.

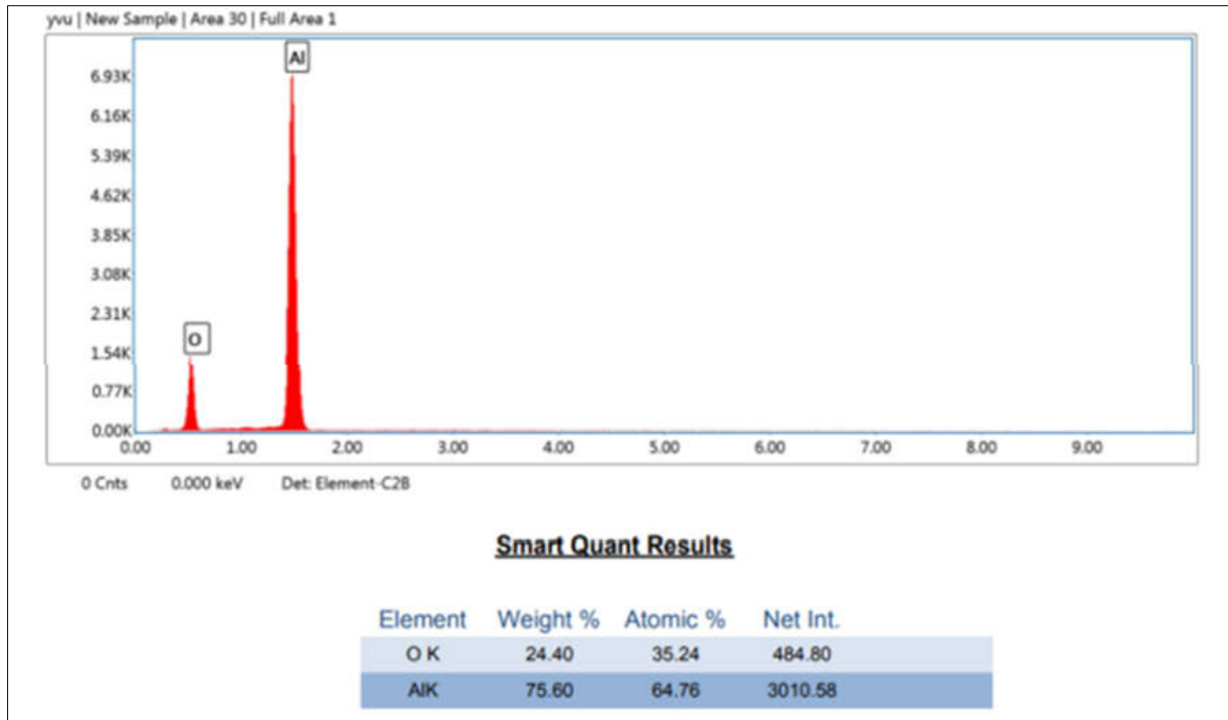


Figure 5 Sample 1 EDX analysis

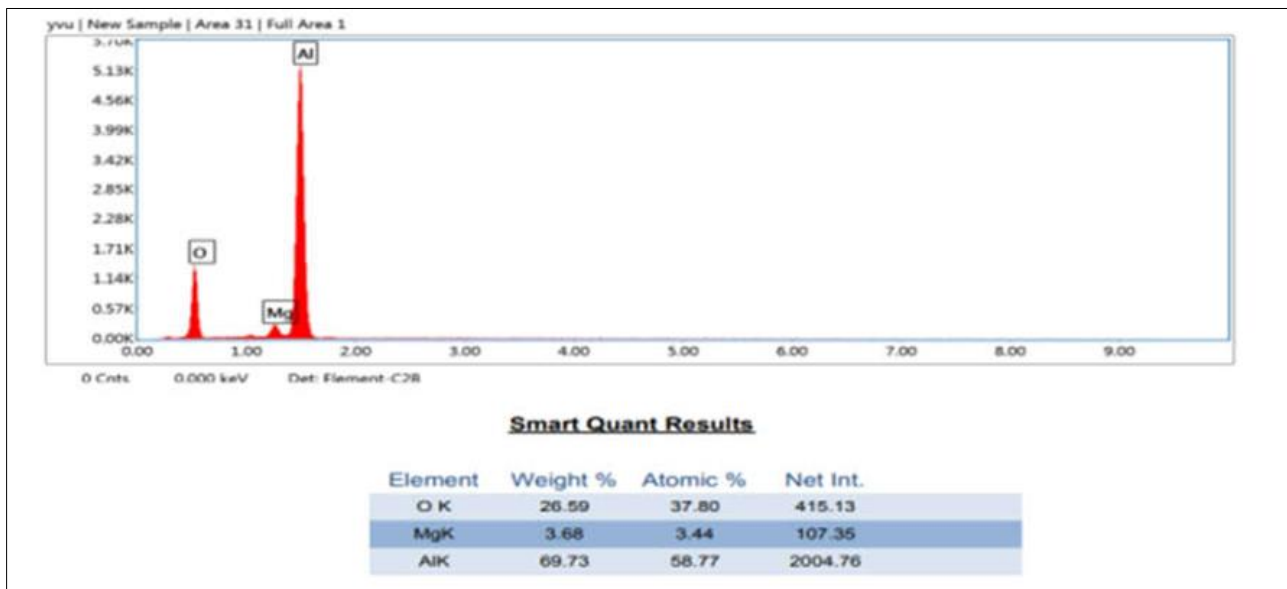


Figure 6 Sample 2 EDX analysis



Figure 7 Sample 3 EDX analysis



Figure 8 Sample 4 EDX analysis

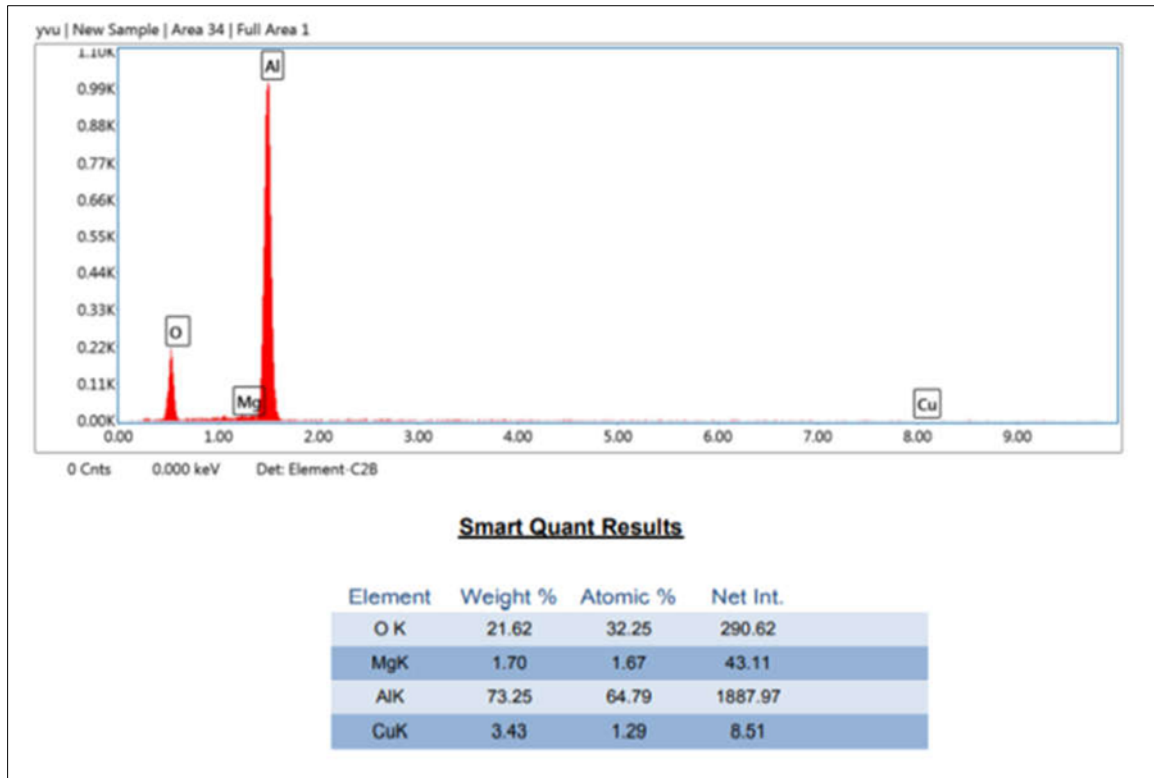


Figure 9 Sample 5 EDX analysis



Figure 10 Sample 6 EDX analysis

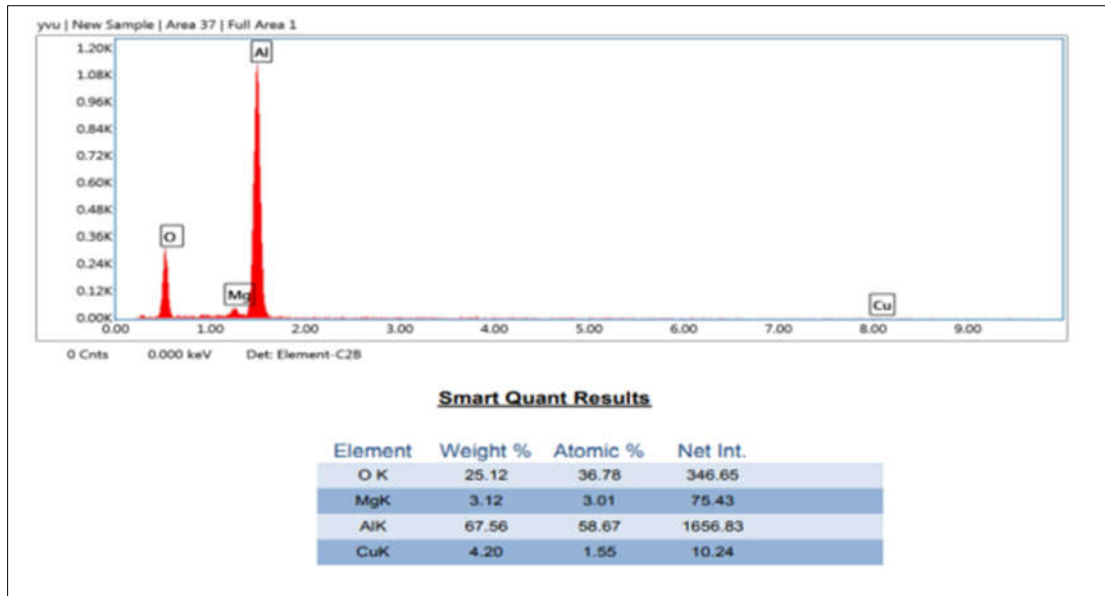


Figure 11 Sample 7 EDX analysis

### 3.6. Analysis of XRD

For the investigation of the crystal structure of materials, X-ray diffraction is used (or alloys). It is evident from the patterns below XRD that every sintered compact has a crystalline structure. It is clear that there is only a slight amount of oxidation and that the crystalline structures of all sintered compacts are the same. Comparing the sintered Al- Mg-Cu compacts to the common JCPDS Card no. 851327 reveals that they likewise contain an FCC structure. Additionally, the XRD graph revealed the discovery of Al-Cu intermetallic compounds, as shown in figure 12.

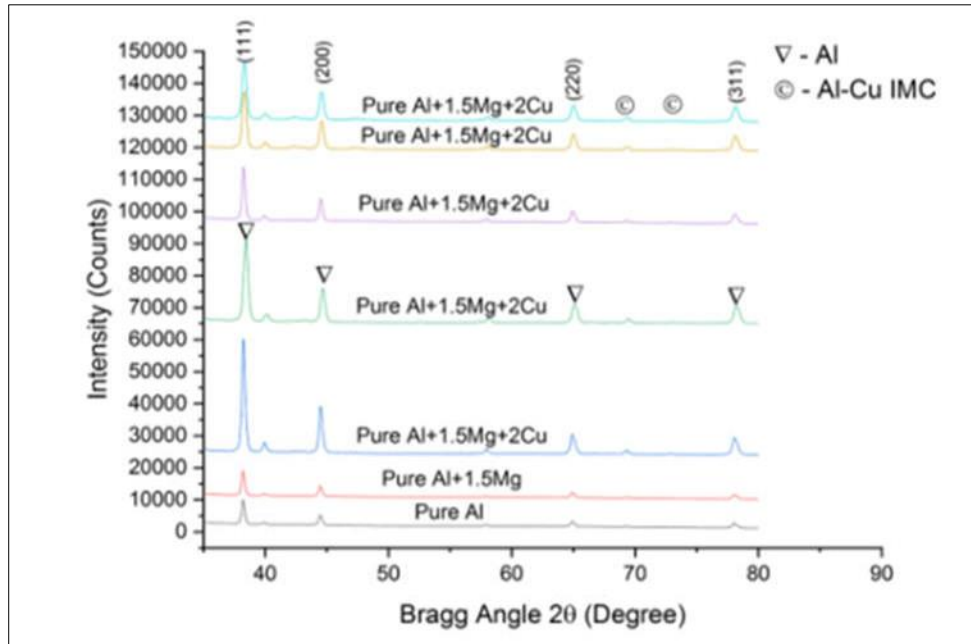


Figure 12 XRD analysis of components

### 3.7. Mechanical Properties

#### 3.7.1. Material Removal Rate

Using a milling machine, the depth of cut and feed rate adjustments yield the material removal rate. It leads to the discovery of the materials' hardness. The rate at which the material is removed is influenced by the material's hardness.

The material removal rate is computed based on the values acquired when varying the feed rate of the components and these values.

**Table 2** Material removal rate values

SAMPLE	Depth of cut(mm)				FEED RATE (mm/min)
	0.5	1	1.5	2.0	
Pure Al	62.5	125	187.5	250	25
Al-1.5%Mg	50	100	150	200	20
Al- 1.5%Mg - 2%Cu	50	100	150	200	20
Al- 1.5%Mg -3%Cu	37.5	75	112.5	150	15
Al- 1.5%Mg -4%Cu	37.5	75	112.5	150	15
Al- 1.5%Mg -5%Cu	25	50	75	100	10
Al- 1.5%Mg -6%Cu	25	50	75	100	10

### 3.7.2. Surface Roughness

A surface roughness tester is used to measure the surface roughness. Surface roughness, measured at each depth of sample cutting. In sample 1, the maximum surface roughness is attained at a cut depth of 1.0 mm. Sample 5's surface roughness is obtained at the lowest level at a cut depth of 0.5 mm, as indicated in Table 3.

**Table 3** Surface roughness values for machined components

SAMPLE	SURFACE ROUGHNESSVALUE ( $\mu\text{m}$ )	DEPTH OF CUT (mm)			
		0.5	1	1.5	2.0
Pure Al	R1	3.36	6.73	5.47	5.88
Al-1.5%Mg	R2	1.83	3.72	5.55	4.16
Al- 1.5%Mg - 2%Cu	R3	1.38	2.69	3.53	2.73
Al- 1.5%Mg -3%Cu	R4	2.28	2.36	2.42	4.13
Al- 1.5%Mg -4%Cu	R5	1.30	4.01	2.08	3.56
Al- 1.5%Mg -5%Cu	R6	1.38	2.79	2.29	2.34
Al- 1.5%Mg -6%Cu	R7	1.57	3.63	3.63	2.68

## 4. Conclusion

The aforesaid research work led to the following conclusions, which are drawn: The composition of the elements determines the thickness of the aluminium 2024 powder metallurgical materials. When comparing green density with sintered density, the density was also lessened. Compared to sintered compacts, green compacts have higher levels of porosity and oxidation. The alloy composition is mounted on the material proportion. The FCC structure was discovered during XRD analysis of all compacts. Sample 1 had the most surface roughness, which were 6.73. Material structure affects a material's hardness.

## Compliance with ethical standards

### Acknowledgments

We are expressing our gratitude to the principal and all the staff of the JNTUA College of Engineering in Pulivendula for providing the resources and assistance we needed to complete the project. We thank all my friends, who helped us directly or indirectly during our course of research work and in person.

*Disclosure of conflict of interest*

No authors have conflict of interest.

---

**References**

- [1] M. Abdel-Rahman and M. N. El-Sheikh, "Workability in forging of powder metallurgy compacts," *Journal of Materials Processing Tech.*, vol. 54, no. 1–4, pp. 97–102, 1995, doi: 10.1016/0924-0136(95)01926-X.
- [2] R. W. Cooke, R. L. Hexemer, I. W. Donaldson, and D. P. Bishop, "Press-and-sinter processing of a PM counterpart to wrought aluminum 2618," *Journal of Materials Processing Technology*, vol. 230, pp. 72–79, 2016, doi: 10.1016/j.jmatprotec.2015.11.011.
- [3] G. A. Sweet, R. L. Hexemer, I. W. Donaldson, A. Taylor, and D. P. Bishop, "Powder metallurgical processing of a 2xxx series aluminum powder metallurgy metal alloy reinforced with AlN particulate additions," *Materials Science and Engineering A*, vol. 755, no. April, pp. 10–17, 2019, doi: 10.1016/j.msea.2019.03.122.
- [4] M. T. Jia, J. M. Liang, D. L. Zhang, C. Kong, and B. Gabbitas, "Effects of holding time during pre-sintering and post-forging annealing on the microstructure and mechanical properties of Ti parts fabricated by powder compact forging," *Materials Science and Engineering A*, vol. 655, pp. 113–121, 2016, doi: 10.1016/j.msea.2015.12.079.
- [5] R. E. D. Mann, R. L. Hexemer, I. W. Donaldson, and D. P. Bishop, "Hot deformation of an Al-Cu-Mg powder metallurgy alloy," *Materials Science and Engineering A*, vol. 528, no. 16–17, pp. 5476–5483, 2011, doi: 10.1016/j.msea.2011.03.081.
- [6] G. A. W. Sweet *et al.*, "Microstructural evolution of a forged 2XXX series aluminum powder metallurgy alloy," *Materials Characterization*, vol. 151, no. February, pp. 342–350, 2019, doi: 10.1016/j.matchar.2019.03.033.
- [7] K. H. Min, S. P. Kang, D. G. Kim, and Y. Do Kim, "Sintering characteristic of Al<sub>2</sub>O<sub>3</sub>-reinforced 2xxx series Al composite powders," *Journal of Alloys and Compounds*, vol. 400, no. 1–2, pp. 150–153, 2005, doi: 10.1016/j.jallcom.2005.03.070.
- [8] R. Seetharam, S. K. Subbu, and M. J. Davidson, "Hot workability and densification behavior of sintered powder metallurgy Al-B<sub>4</sub>C preforms during upsetting," *Journal of Manufacturing Processes*, vol. 28, pp. 309–318, 2017, doi: 10.1016/j.jmapro.2017.06.012.
- [9] R. Chandramouli, T. K. Kandavel, D. Shanmugasundaram, and T. Ashok Kumar, "Deformation, densification, and corrosion studies of sintered powder metallurgy plain carbon steel preforms," *Materials and Design*, vol. 28, no. 7, pp. 2260–2264, 2007, doi: 10.1016/j.matdes.2006.05.018.
- [10] L. P. Lefebvre, Y. Thomas, and B. White, "Effects of lubricants and compacting pressure on the processability and properties of aluminum P/M parts," *Journal of Light Metals*, vol. 2, no. 4, pp. 239–246, 2002, doi: 10.1016/S1471-5317(03)00007-5.
- [11] M. A. Jabbari Taleghani, E. M. Ruiz Navas, and J. M. Torralba, "Microstructural and mechanical characterisation of 7075 aluminium alloy consolidated from a premixed powder by cold compaction and hot extrusion," *Materials and Design*, vol. 55, pp. 674–682, 2014, doi: 10.1016/j.matdes.2013.10.028.